Codon optimization, expression in *Escherichia coli*, and immunogenicity analysis of deformed wing virus (DWV) structural protein

Dongliang Fei [1, 2] , **Yaxi Guo** [1] , **Qiong Fan** [3] , **Ming Li** [2] , **Li Sun** [2] , **Mingxiao Ma** [2] , **Yijing Li** [Corresp. 1]

[1] College of Veterinary Medicine, Northeast Agricultural University, Haerbin, Heilongjiang, China

[2] Laboratory Animal Center, Jinzhou Normal University, Jinzhou, Liaoning, China

[3] Jinzhou Agricultural and Rural Comprehensive Service Center, Jinzhou, Liaoning, China

Corresponding Author: Yijing Li
Email address: 371751697@qq.com

Background: Deformed wing virus (DWV) is a serious threat to honey bees (*Apis mellifera*) and is considered a major cause of elevated losses of honey bee colonies. However, lack of information on the immunogenicity of DWV structural proteins has hindered the development of effective biocontrol drugs. **Methods:** We optimized the *VP1*, *VP2*, and *VP3* codons of DWV surface capsid protein genes on the basis of an *Escherichia coli* codon bias, and the optimized genes of *roVP1*, *roVP2*, and *roVP3* were separately expressed in *E. coli* and purified. Next, the three recombinant proteins of *roVP1*, *roVP2*, and *roVP3* were intramuscularly injected into BALB/c, and the immunogenicity was evaluated by the levels of specific IgG and cytokines. Furthermore, anti-*roVP*-antisera (*roVP1* or *roVP2* or *roVP3*) from the immunized mice was incubated with DWV for injecting healthy white-eyed pupae for the viral challenge test, respectively. **Results:** The optimized genes *roVP1*, *roVP2*, and *roVP3* achieved the expression in *E. coli* using SDS-PAGE and Western blotting. Post- immunization, *roVP2* and *roVP3* exhibited higher immunogenicity than *roVP1* and stimulated a stronger humoral immune response in the mice, which showed that the recombinant proteins of *roVP3* and *roVP2* induced a specific immune response in the mice. In the challenge test, data regarding quantitative real-time RT-PCR (qRT-PCR) from challenged pupae showed that the level of virus copies in the recombinant protein groups was significantly lower than that of the virus-only group at 96 h post-inoculation (*P* < 0.05). Among them, the degree of neutralisation using antibodies raised to the recombinant proteins are between approximately 2-fold and 4-fold, and the virus copies of the *roVP3* group are the lowest in the three recombinant protein groups, which indicated that specific antibodies against recombinant proteins *roVP1*, *roVP2*, and *roVP3* of DWV could neutralize DWV to reduce the virus titer in the pupae. Collectively, these results demonstrated that the surface capsid protein of DWV acted as candidates for

the development of therapeutic antibodies against virus.

1 **Title: Codon optimization, expression in *Escherichia coli*, and**

2 **immunogenicity analysis of deformed wing virus (DWV) structural**

3 **protein**

10 **Author:** Dongliang Fei [1,2], Yaxi Guo[2], Qiong Fan[3], Ming Li[2], Li Sun[2], Mingxiao Ma[2], Yijing

11 Li[1]*

12 *** Corresponding Author:**

13 Yijing Li   **E-mail:** 371751697@qq.com

14 **Author's Institution:** 1. College of Veterinary Medicine, Northeast Agricultural University,

15 Haerbin, Heilongjiang, China; 2. Laboratory Animal Center, Jinzhou Medical University,

16 Jinzhou, Liaoning, China; 3. Jinzhou Agricultural and Rural Comprehensive Service Center,

17 Jinzhou, Liaoning, China

18 **Tel.:** +86-13704061657

19 **Fax:** +86-04164673265

Codon optimization, expression in *Escherichia coli*, and immunogenicity analysis of deformed wing virus (DWV) structural protein

ABSTRACT:

Background: Deformed wing virus (DWV) is a serious threat to honey bees (*Apis mellifera*) and is considered a major cause of elevated losses of honey bee colonies. However, lack of information on the immunogenicity of DWV structural proteins has hindered the development of effective biocontrol drugs.

Methods: We optimized the *VP1*, *VP2*, and *VP3* codons of DWV surface capsid protein genes on the basis of an *Escherichia coli* codon bias, and the optimized genes of *roVP1*, *roVP2*, and *roVP3* were separately expressed in *E. coli* and purified. Next, the three recombinant proteins of *roVP1*, *roVP2*, and *roVP3* were intramuscularly injected into BALB/c, and the immunogenicity was evaluated by the levels of specific IgG and cytokines. Furthermore, anti-*roVP*-antisera (*roVP1* or *roVP2* or *roVP3*) from the immunized mice was incubated with DWV for injecting healthy white-eyed pupae for the viral challenge test, respectively.

Results: The optimized genes *roVP1*, *roVP2*, and *roVP3* achieved the expression in *E. coli* using SDS-PAGE and Western blotting. Post- immunization, *roVP2* and *roVP3* exhibited higher immunogenicity than *roVP1* and stimulated a stronger humoral immune response in the mice, which showed that the recombinant proteins of *roVP3* and *roVP2* induced a specific immune response in the mice. In the challenge test, data regarding quantitative real-time RT-PCR (qRT-PCR) from challenged pupae showed that the level of virus copies in the recombinant protein groups was significantly lower than that of the virus-only group at 96 h post-inoculation ($P < 0.05$). Among them, the degree of neutralisation using antibodies raised to the recombinant proteins are between approximately 2-fold and 4-fold, and the virus copies of the *roVP3* group are the lowest in the three recombinant protein groups, which indicated that specific antibodies against recombinant

51 proteins *roVP1*, *roVP2*, and *roVP3* of DWV could neutralize DWV to reduce the
52 virus titer in the pupae. Collectively, these results demonstrated that the surface
53 capsid protein of DWV acted as candidates for the development of therapeutic
54 antibodies against virus.

55 **Keywords:** DWV; Codon optimization; Structural proteins; Immune responses;
56 Challenge test.

57

58 **BACKGROUND**

59 The western honey bee (*Apis mellifera*) is an important insect species for the
60 commercial pollination of high-value crops and plays a crucial role in agricultural
61 ecology (*Garibaldi et al., 2013; Škubník et al., 2017*). However, as highlighted by
62 the elevated losses of honey bee colonies in major beekeeping regions owing to
63 colony collapse disorder, annual declines in honey bee populations have
64 significantly increased over the past two decades (*De Smet et al., 2012*). Multiple
65 explanations for colony losses have been proposed, including habitat degradation
66 and the effects of pathogens, parasites, and pesticides (*Tehel et al., 2019*). Of the
67 numerous infectious pathogens and infesting parasites, *Varroa destructor*, an
68 ectoparasitic mite, and deformed wing virus (DWV) are regarded as serious threats
69 to honey bee health and survival (*Budge et al., 2015; Natsopoulou et al., 2017*).
70 DWV, often considered among the most common and prevalent viruses in honey
71 bee colonies (*Dalmon et al., 2017; Gisder et al., 2018*), was originally isolated
72 from a sample of symptomatic honey bees during the early 1980s in Japan;
73 currently, DWV is distributed worldwide, wherever *Varroa* mites are found
74 (*Bailey et al., 1991*). DWV infection induces clinical symptoms that include
75 deformed and crippled wings, discoloration and paralysis, and a generally
76 shortened lifespan (*De Miranda et al., 2010*). DWV is a positive -strand RNA
77 virus belong to the family *Iflaviridae* of the order *Picornavirales* (*Lanzi et al.,*
78 *2006*). DWV is separated into three major variants: DWV-A, -B, and -C (*Mordecai*
79 *et al., 2016*). The International Committee on Taxonomy of Viruses recognizes
80 two master variants of DWV-A—DWV and Kakugo virus—whereas DWV-B

81   contains *Varroa destructor* viruses, and DWV-C, which has only recently been
82   described, is phylogenetically distinct from both A and B types (*Gisder et al.,*
83   *2016; Mordecai et al., 2016*). DWV has a single-stranded RNA genome of
84   approximately 10,000 nucleotides, and the whole genome encodes one large,
85   uninterrupted open-reading frame that is translated into polyproteins that are
86   cleaved by viral proteases to produce structural and nonstructural proteins (*Bowen-*
87   *Walker et al., 1999*). The three major structural proteins VP1, VP2, and VP3 from
88   one polyprotein precursor form a protomer, an elementary building block of the
89   virus capsid (*Škubník et al., 2017, Koziy et al., 2019*).
90   Although DWV is regarded as one of the primary viruses that are associated with
91   honeybee colony losses (*Francis et al, 2013*), the effective medicine and method
92   against DWV remain limited. Antibodies, as naturally occurring proteins, play an
93   important role in neutralizing virus; thus, they have been widely utilized in the
94   prevention and control of epidemic diseases as well as for research purposes (*Hu et*
95   *al., 2019; Nieuwkoop et al., 2019*). The capability of virus neutralization and
96   antibodies titers primarily depends on antigenic immunogenicity. It is crucial to
97   identify an excellent immunogenic antigen for developing therapeutic antibodies.
98   A previous study has demonstrated that viral structural proteins not only play an
99   important role in viral infection but also possess superior immunogenicity in
100   producing neutralizing antibodies (*Ojha et al., 2019; Xie et al., 2019; Mahdy et al.,*
101   *2019*); we thus speculate that the three major DWV proteins have possibly been
102   suitable targets for effective therapeutic antibody against DWV. Presently, the VP1
103   recombinant fragment protein of DWV has already been successfully
104   recombinantly expressed and used for the generation of monoclonal antibodies
105   (*Lamp et al., 2016*); however, limited studies on their antigenic differences of the
106   three structural proteins have restricted the development of therapeutic drugs.
107   In the present study, we obtained the recombinant proteins *roVP1, roVP2,* and
108   *roVP3* of DWV in *E. coli* using bioinformatics-based codon optimization; next,
109   BALB/c mice were immunized with the recombinant proteins, and the
110   immunogenicity of the three recombinant proteins was evaluated on the basis of
111   the specific antibody level, lymphocyte proliferation, and cytokine expression.
112   Furthermore, the challenge test was performed to assess the virus‐neutralizing

113 ability of anti-*roVP*-antisera (*roVP1* or *roVP2* or *roVP3*). To the best of our
114 knowledge, this is the first study to express DWV structural protein genes and
115 evaluate their immunogenic potential.

116

MATERIALS AND METHODS

Ethics statement and animal care

119 All animal experiments were performed in accordance with the ethical guidelines
120 of Jinzhou Medical University, and the research protocol was approved by the
121 Animal Care and Use Committee of Jinzhou Medical University (Approval
122 number: 2018-012). The animal facility and rearing condition was based on
123 laboratory animal environment and facilities (GB14925-2010) and laboratory
124 animal feed nutrient standard (GB14924.3-2010) of China. The mice were
125 sacrificed by carbon dioxide (CO_2) inhalation.

126

Strains, plasmids, virus, and antibody

128 *E. coli* DH5α and BL21 (DE3) pLysS strains were purchased from TranGen
129 Biotech (Beijing, China). The vector pET-28a was obtained from Novagen (San
130 Diego, CA). DWV LN8/17 strain (accession number, MF770715) was isolated,
131 identified, purified, and preserved at the author's laboratory, and the purification
132 method of DWV particles was essentially described by Lamp *et al.* (*Lamp et al.,*
133 *2016*). 6*His-tag antibody was purchased from Proteintech Group, Inc (Wuhan,
134 China), and horseradish peroxidase (HRP)-labeled goat anti-mouse immunoglobin
135 G (IgG) was obtained from Bioss ANTIBODIES (Beijing, China).

136

Amplification and cloning

138 Using a TIAamp viral RNA kit (TIANGEN, China), viral RNA was extracted from
139 the purified DWV LN8/17 strain at our laboratory (MF770715). Next, first-strand
140 complementary DNA (cDNA) was transcribed using EasyScript cDNA Synthesis
141 SuperMix (TranGen Biotech, China), according to the manufacturer's instructions.
142 DWV *VP1, VP2,* and *VP3* were amplified using polymerase chain reaction (PCR)
143 with specific primers designed based on the nucleotide sequence of the DWV
144 LN8/17 strain (*VP1,* forward primer: 5'-ATCGTATATTAAATTTRGCAGAGG-

145 3', reverse primer: 5'-GGAGAGCCAGCAGAACC-3'; *VP2*, forward primer: 5'-
146 AACAAGGACCTGGTAAGGTAAGTA-3',   reverse   primer: 5'-
147 TTATCCTAAAGTCACAAAAA-3';   VP3,   forward   primer: 5'-
148 CAGTGCAGGCAAAACCAGAGATG-3',   reverse   primer: 5'-
149 CGGGACAAAATGGCGAGGAG-3'). PCR was conducted as follows: initial
150 denaturation at 95°C for 5 min; 25 cycles at 95°C for 45 s and 55°C for 40 s (*VP1*),
151 51°C for 40 s (*VP2*), or 50°C for 40 s (*VP3*); 72°C for 60 s; and final extension for
152 10 min at 72°C. The PCR products were inserted into a pMD18-T cloning vector
153 and sequenced using Synbio Techology Corporation (Suzhou, China).

154

155 **Codon optimization and construction of recombinant expression**
156 **vectors**
157 *VP1*, *VP2*, and *VP3* sequences of the DWV LN8/17 strain were analyzed and
158 optimized based on *E. coli*-preferred codons without changing the amino acid
159 sequence of the corresponding proteins (*Gao et al., 2015; Mansouri et al., 2013;*
160 *Wang et al., 2012*). High-frequency-usage codons in *E. coli* were the most
161 commonly used for each of the individual amino acids (*Tian et al., 2017*). *VP1*,
162 *VP2*, and *VP3* were subsequently reverse-translated by applying the single-most
163 commonly used codon for each amino acid such that the final codon-optimized
164 genes were represented by the most likely nondegenerate coding sequence, and
165 online   optimization   software   (http://www.jcat.de/   and
166 http://genomes.urv.es/OPTIMIZER/) were utilized for codon design. The designed
167 genes *roVP1*, *roVP2*, and *roVP3* were synthesized by Synbio Techology
168 Corporation (Suzhou, China) and inserted into the plasmid pET-28a(+) with the
169 respective restriction enzymes (*roVP1*: BamH I and Hind III; *roVP2*: EcoR I and
170 Hind III; and *roVP3*: BamH I and Hind III), and the 6× His tag sequence is located
171 at the N terminus of the recombinant plasmids.

172

173 **Protein expression and purification**
174 For each protein, BL21 (DE3) pLysS cells were transformed with the appropriate
175 recombinant plasmids and plated on LB agar with 50 μg/mL kanamycin. The
176 transformed BL21 cells were incubated at 37°C in an orbital shaker at 220 rpm

177 until an OD_{600} of 0.6 was obtained and then induced with 0.1 mM, 0.25 mM, or 0.5

178 mM isopropyl-β-D-thiogalactoside (IPTG; Sigma-Aldrich, St. Louis, MO, USA) at

179 30°C for 6 h. To verify the expression of the target proteins, the cells were

180 collected by centrifugation and the target proteins were confirmed using 12%

181 sodium dodecyl sulfate polyacrylamide gel electrophoresis (SDS-PAGE).

182 For purifying the recombinant proteins, the cultures were harvested by

183 centrifugation at 6,000 rpm for 30 min at 4°C, and the obtained cell pellets were

184 stored at −80°C for later use. All recombinant proteins in inclusion bodies were

185 purified and collected using Ni-affinity chromatography (GE Healthsystems,

186 Uppsala, Sweden), according to the manufacturer's instructions. Briefly, the

187 inclusion bodies were solubilized in 6 M urea after being washed twice with a

188 washing buffer (1000 mL of 4 M urea, 1% Triton X-100, 5 mM EDTA, 5 mM β-

189 mercaptoethanol, and 50 mM Tris-HCl; pH 8.5) at room temperature for 30 min.

190 The purified and denatured proteins were then refolded via dialysis in phosphate

191 buffered saline (PBS) containing urea (initial concentration: 6 M; decreased by 1

192 M/dialysis) and 0.5 M arginine. The refolded proteins were then dialyzed five

193 times against the dialysis buffer to eliminate arginine, changing from 0.5 M to 0 M

194 buffers by the 12 h time-point. Recombinant *roVP1*, *roVP2*, and *roVP3* proteins

195 were confirmed using SDS-PAGE and Western blotting and stored at −80 °C until

196 further use.

197

198 **Western blot analysis**

199 The purified recombinant proteins were electrophoresed on 12% polyacrylamide

200 slabs along with pre-stained protein markers on adjacent lanes and transferred to a

201 polyvinylidene difluoride (PVDF) membrane. The membranes were blocked

202 overnight with 3% (w/v) skim milk in Tris-buffered saline containing 0.05%

203 Tween-20 (TBST) at 4°C overnight, then incubated for 1 h at room temperature

204 with an anti–His tag antibody (1:3000) or an anti-DWV polyclonal antibody (1:500)

205 in blocking buffer. The anti-DWV polyclonal antibody was obtained from the mice

206 after they were injected thrice at biweekly intervals with the purified virus particles

207 of DWV. Simultaneously, the serum of healthy mice was also used as the negative

208 control for incubating with PVDF membrane of the recombinant proteins. After

209 three washes, the membranes were incubated with HRP-labeled goat anti-mouse
210 IgG (1:3000) for 2 h at room temperature. After three 5-min washes with TBST,
211 color development was performed with an ECL Western substrate (Thermo
212 Scientific, USA).

213

214 **Mice immunizations**
215 To evaluate the immunogenicity of the recombinant proteins, 4–6-week-old female
216 BALB/c mice (five/group) were subcutaneously immunized with a mixture of 200
217 μL each of the purified protein (20 μg) and 200 μL of Freund's incomplete
218 adjuvant (Sigma). All mice were then boosted twice with the same dose of
219 Freund's incomplete adjuvant at a 2-week interval with the same recombinant
220 proteins. Negative controls were injected with PBS, and positive controls with
221 purified virus particles. Serum samples were prepared prior to the first
222 immunization and 2 weeks after each immunization and stored at -80°C until
223 further analysis. At 2 weeks after the last inoculation, the animals were sacrificed
224 by euthanasia to isolate splenocytes for lymphocyte proliferation in response to the
225 recombinant proteins.

226

227 **Detection of specific antibody responses using enzyme-linked immunosorbent**
228 **assay (ELISA)**
229 According to a previously reported method, IgG levels in mice sera were detected
230 using ELISA (*Stachyra et al., 2016*). In brief, microtiter plates (Corning, USA)
231 were coated with 50 μL of the purified virus particles/well at a concentration of 5
232 μg/mL at 4°C overnight. The plates were washed thrice with PBS containing 0.05%
233 TBST and blocked with 2% bovine serum albumin (BSA)–PBST for 1.5 h at 37°C.
234 After five washes, the sera samples (1:200) were added, and the plates were
235 incubated for 1.5 h at 37°C. After another five washes with PBST, the plates were
236 incubated for 1 h at 37°C with HRP-conjugated goat anti-mice IgG (1:3000). After
237 a final round of washes, the products were detected by adding the developing
238 reagent tetramethylbenzidine. Absorbance was read at a wavelength of 450 nm
239 (OD_{450}) using an ELx808 Absorbance Microplate Reader (BioTek Instruments,
240 USA).

241

Lymphocyte proliferation assays and cytokine detection

242 Two weeks after the last immunization, spleens were harvested from five mice in
243 each group under sterile conditions. Splenocyte suspensions were prepared, and the
244 splenocytes were cultured in 96-well plates at a density of 2.0×10^6 cells/well in
245 Dulbecco's modified Eagle's medium containing 10% fetal bovine serum. The
246 cells were then stimulated with the purified virus particles (10 μg/mL), and
247 Dulbecco's modified Eagle's medium was used alone as the negative control.
248 According to the manufacturer's instructions, the plates were incubated in 5% CO_2
249 for 24 h at 37°C, and then a cell-counting kit 8 solution (Vazyme, China) was
250 added to each well and incubated for 8 h followed by the addition of 150 μL
251 dimethyl sulfoxide solution per well; absorbance was measured at 450 nm with a
252 microplate reader. Stimulation index (SI) was calculated as the ratio of the OD_{450}
253 of the stimulated cells to the OD_{450} of the negative controls. The cytokine levels of
254 interleukin (IL)-2, IL-4, IL-10, and interferon gamma (IFN-γ) from serum samples
255 were detected using a commercial ELISA kit (Dakewei, China), according to the
256 manufacturer's instructions.

258

Challenge test in the honeybee pupae

259 For preliminarily assessing the ability of IgG antibodies from mice immunized
260 using the recombinant proteins to neutralize DWV, we collected mice serum of the
261 groups after the third immunization to perform the challenge test. The challenge
262 test was modified with reference to Tehel's and Sun's methods (*Sun et al., 2018;*
263 *Tehel et al., 2019*). Prior to the challenge test, DWV were incubated with anti-
264 *roVP1*- antisera, anti-*roVP2*-antisera, anti-*roVP3*-antisera, or anti-DWV-antisera
265 (the mice immunized with DWV viral particles, and virus purification were
266 performed as per Lamp's description (*Lamp et al., 2016*)) for 1 h at 37 ℃. A total
267 of 30 healthy white-eyed pupae from the same colony in Wendilou Town of
268 Jinzhou (41.25°N, 121.11°E), were randomly distributed into six groups, with each
269 group containing 5 pupae. Next, the pupae were transferred to 48-well microtiter
270 plates, and each pupa in groups 1-4 was injected with 1 μL of virus particles and
271 antisera suspension containing 1×10^4 copies of DWV and 50-diluted antisera; the

273 pupae of group 5 were only injected with a mixture of five antisera from the
274 immunized mice, and the pupae of group 6 were only injected with 1×10^4 virus
275 particles, and all the groups were maintained in incubators at 35 ℃ and 50% RH
276 to monitor pupal development. At 96 h post-inoculation (p.i.), all pupae of the
277 groups were collected, then total RNA extraction was performed according to the
278 manufacturer's instructions (TranGen, China), and the extracts were stored at -80 ℃
279 until further use.
280 The quantification of the DWV titer in the samples was performed using real time
281 qRT-PCR using the *TransScript®* Green One-Step qRT-PCR SuperMix (TranGen,
282 China), and RT-qPCR reaction contained 75 ng RNA*,* $1 \times$*TransScript®* Tip Green
283 qPCR SuperMix, $1 \times$ Passive Reference Dye, and 5 pmol of each primer: DWV-F1
284 and DWV-R1   (DWV-F1:5'-TAGTGCTGGTTTTCCTTTGTC-3'; DWV-R1:5'-
285 CTGTGTGAGTAATTGAATCTC-3') with Actin F1 and R1 (Actin-F1:5'-
286 CTTGGAATCGCAGATAGAATGC-3';   Actin-R1:5'-
287 AATTTTCATGGTGGATGGTGC-3') as the reference gene. *Apis mellifera β-*
288 actin, which is reported as a stable reference gene in the DWV infection, was used
289 for normalization as described by Chen (*Chen et al., 2005*). The qPCR protocol for
290 both DWV and β-actin reference gene was as follows: 45°C for 5 min, 95°C for 30
291 sec, 40 cycles of 95°C for 5 sec, 54°C for 30 sec (DWV), 55°C for 30 sec (β-actin),
292 and 72°C for 20 sec. The relative DWV titers of the pupae were assessed by
293 calculating delta Ct values ($\Delta Ct = Ct_{(DWV)} - Ct_{(actin)}$).
294 **Statistical analysis**
295 All data are expressed as mean ± standard deviation. Statistical analyses were
296 performed using GraphPad Prism 7.0 software (GrapPad, USA). Differences in the
297 levels of antibodies, lymphocyte proliferation, and cytokines among the various
298 groups were evaluated using an independent samples t-test. $P < 0.05$ was
299 considered statistically significant.
300
301 **RESULTS**
302 **Codon optimization of *VP1*, *VP2*, and *VP3***
303 After sequencing, the full lengths of *VP1*, *VP2*, and *VP3* were 1248, 675, and 738
304 bp, encoding polypeptide of 416, 225, and 246 amino acid residues, respectively.

305   Analysis of three structural protein genes revealed various rare codons, including
306   CTT (Leu), CTA (Leu), CGA (Arg), AGA (Arg), AGG (Arg), GGA (Gly), ATA
307   (Ile), CCC (Pro), TCA (Ser), and ACA (Thr) in *E. coli*. To obtain high expression
308   level of the recombinant VP1, VP2, and VP3 proteins, *roVP1*, *roVP2*, and *roVP3*
309   were synthesized so as to replace the low-frequency-usage codons with high-
310   frequency ones in *E. coli*. Results indicated that 71% (298/416; *roVP1*), 72%
311   (162/225; *roVP2*), and 73% (180/246; *roVP3*) of the codons were optimized
312   according the codon bias of the *E. coli* genome (**Table S1**). The sequence
313   alignment showed that codon-optimized *roVP1*, *roVP2*, and *roVP3* shared 72.8%,
314   72.6%, and 71.4% identity with wild-type *VP1*, *VP2*, and *VP3*. Furthermore, the
315   codon adaptation index (CAI) of the three genes increased from 0.19, 0.20, and
316   0.19 to 0.94, 0.95, and 0.94 **(Figure S1)**, respectively; further, the GC content was
317   also adjusted from 41%, 38%, and 39% to 56%, 55%, and 53%, respectively. The
318   substitution of nucleotides did not alter their coding amino acid sequences.

319

320   **Expression and purification of the recombinant proteins**

321   The recombinant plasmids containing *roVP1*, *roVP2*, and *roVP3* were transformed
322   into *E. coli* BL21 (DE3) and expressed under the induction of IPTG. The
323   recombinant proteins roVP1 and roVP3 were expressed in a soluble form and
324   purified from the supernatant. The recombinant protein roVP2 was expressed in an
325   insoluble form, i.e., as inclusion bodies, and was purified after solubilization in 6
326   M urea and by using Ni-affinity chromatography. SDS-PAGE analysis showed that
327   the apparent molecular weights of the recombinant proteins were approximately
328   50.5 (*roVP1*), 29.1 (*roVP2*), and 32.6 kDa (*roVP3*), which was in accordance with
329   their theoretical values (**Figure 1**). The optimized IPTG concentrations of
330   expression were 0.5 (*roVP1*: **Figure 1A, lane 3**), 0.1 (*roVP2*: **Figure 1B, lane 1**),
331   and 0.25 (*roVP3*: **Figure 1C, lane 2**) mmol/L. After purification with Ni-affinity
332   chromatography, the recombinant proteins were presented as a single band (*roVP1*:
333   **Figure 1A, lane 5**; *roVP2*: **Figure 1B, lane 5**; *roVP3*: **Figure 1C, lane 5**).

334

335   **Western blot analysis of the recombinant proteins**

336 To determine the expression of the recombinant proteins, Western blot analysis
337 was performed using mouse anti–His tag antibodies and anti-DWV polyclonal
338 antibodies, but the recombinant proteins didn't combine with the negative
339 control (the serum of healthy mice). The results showed that the single reaction
340 bands corresponding to the bands in SDS-PAGE could be observed in the PVDF
341 membrane, indicating the reactogenicity of the recombinant proteins *roVP1*, *roVP2*,
342 and *roVP3* to specific antibodies (**Figure 2 A-C, Figure S2**).

343

344 **Immune effect comparison for serum antibody titers**
345 To evaluate the immunogenicity of the recombinant proteins, BALB/c mice were
346 immunized with *roVP1*, *roVP2*, or *roVP3* thrice at 2-week intervals and the total
347 IgG antibody levels were measured using ELISA. As shown in **Figure 3 and**
348 **Table S2**, after the first immunization, serum total IgG levels were higher in mice
349 of the recombinant groups and group of the purified virus particles than in those of
350 the control group ($P < 0.05$). In addition, the mice that were inoculated with the
351 purified virus particles induced higher levels of IgG antibodies than those of the
352 other groups. After the booster immunization, the antibody levels in group *roVP3*
353 were significantly higher than those in the *roVP2* and *roVP1* groups; the *roVP1*
354 group induced the lowest immune response. At 2 weeks after the last immunization,
355 high levels of IgG were detected in the three recombinant protein groups compared
356 with those in the control PBS group ($P < 0.05$). Although the difference between
357 the *roVP3* and *roVP2* groups was insignificant ($P > 0.05$), the antibody levels were
358 higher in the *roVP3* group than in the *roVP2* group, and both of them were
359 significantly higher than those in the *roVP1* group ($P < 0.05$). These results
360 suggest that the three recombinant proteins had strong immunogenicity and that
361 roVP3 effectively promoted the antibody levels induced in mice.

362

363 **Immune effect comparison for lymphocyte proliferation and cytokine**
364 **secretion**
365 To evaluate splenocyte proliferation *in vitro*, spleen cell suspensions from the mice
366 of different groups were prepared at two weeks after the last immunization. Our
367 data suggest that a significantly higher SI value was obtained from mice

368   immunized with the recombinant protein groups and from the group of purified
369   virus particles than from the control groups (*P* < 0.05) (**Figure 4, Table S3).**
370   Moreover, the *roVP2* group exhibited the highest level of lymphocyte proliferation
371   (SI=1.96±0.18), which was insignificantly different from that in the *roVP1* and
372   *roVP3* groups; further, lymphocyte proliferation in the *roVP3* group (SI
373   =1.79±0.10) was higher than that in the *roVP1* group (SI=1.72±0.12). These results
374   indicate that the recombinant proteins successfully stimulated the mice to promote
375   lymphocyte proliferation.
376   The levels of serum IL-2, IL-4, IL-10, and IFN-γ in each group are shown in
377   **Figure 5** and **Table S4**. Compared with the PBS control group, the IL-2, IL-4, IL-
378   10, and IFN-γ concentrations in the recombinant protein groups were significantly
379   higher (*P* < 0.05) at 2 weeks after the last immunization. Among the recombinant
380   protein groups, the IL-2 and IFN-γ levels were significantly higher in the *roVP2*
381   group than in the *roVP1* and *roVP3* groups (*P* < 0.05), and the mice immunized
382   with *roVP3* showed significantly higher levels of IL-4 (*P* < 0.05). However, the
383   level of IL-10 was not statistically significantly different in the *roVP1*, *roVP2*, and
384   *roVP3* groups (*P* > 0.05). These results show that immunization with the
385   recombinant proteins induced T-cells to secret multiple cytokines.
386
387   **The result of Challenge test in the honeybee pupae**
388   The aim of challenge test was to evaluate whether antisera against DWV
389   recombinant structural protein could neutralize virus in honeybee pupae. As seen
390   in **Figure 6** and **Table S5**, the DWV levels in the group infected with only virus
391   were significantly higher than other groups, indicating that DWV could massively
392   replicate in the pupae at the 96 h. At the same time, the DWV level in the pupae of
393   the five-antisera-only group was significantly lower than in the pupae of any other
394   treatment groups. From the analysis of qRT-PCR data, DWV was undetectable by
395   qRT-PCR in the group injected with five antisera. Compared with the group
396   injected virus particles, we detected a markedly lower relative normalized virus
397   titer in the anti-*roVP*1/2/3-antisera groups and positive control group (anti-DWV-
398   antisera); all of them significantly differed from the virus particles group (*P* <
399   0.05), suggesting that anti-*roVP*1/2/3-antisera or anti-DWV-antisera could

400 neutralize DWV virus particles. Moreover, the anti-DWV-antisera group showed
401 the lowest virus titer in all groups (**Figure 6 and Table S5**). Among anti-
402 *roVP*1/2/3-antisera groups, the relative virus titer of *roVP3* group was the lowest,
403 and it significantly differed from that in the *roVP1* groups (*P*< 0.05) (**Figure 6,
404 Table S5**). These indicated that specific antibody, which was produced in the mice
405 immunized with the recombinant proteins, could neutralize DWV and reduce the
406 virus titer in the pupae.
407
408 **DISCUSSION**
409 DWV is one of the most prevalent and pathogenic viruses affecting honey bee in
410 the world, and it has been directly linked to colony collapse disorder (*Benaets et al.,*
411 *2017; Jamnikar-Ciglenecki et al., 2018*). At present, research of DWV is being
412 focused on the isolation and sequence analysis of the strains, the epidemiological
413 investigation of the interaction with *Varroa destructor*, and the establishment of a
414 rapid detection method (*Bradford et al., 2017; Kevill et al., 2019; Tehel et al.,*
415 *2019; Zhao et al., 2019*). However, research on therapeutic drugs against DWV is
416 still rare. Egg yolk antibodies known as immunoglobulin Y (IgY) have been
417 widely utilized in the prevention and control of epidemic diseases associated with
418 *Acinetobacter baumannii*, *Vibrio splendidus*, the Dengue virus, noroviruses,
419 rotaviruses, and duck adenovirus 3 (*Fink et al., 2017; Ghosh et al., 2018;*
420 *Jahangiri et al., 2019; Li et al., 2016; Yin et al., 2019*). Moreover, Li sun reported
421 that specific IgY could be obtained from hens immunized with an inactivated
422 Chinese Sacbrood virus (CSBV) vaccine, which has the ability to neutralize CSBV
423 (*Sun et al., 2018*). Therefore, we should be able to develop novel therapeutic drugs
424 against DWV using this strategy. However, owing to lack of an efficient cell
425 culture system and limited animal models for DWVs, we were unable to obtain
426 large amounts of the viral protein to perform further research in this direction. At
427 the same time, the immunogenicity and antigenic differences among the DWV
428 structural proteins remain unclear. In this study, we successfully produced the
429 recombinant DWV proteins *roVP1*, *roVP2*, and *roVP3* via expression in *E. coli* to
430 evaluate their immunogenicity, and Western blot analysis of the recombinant
431 proteins conducted using anti-His monoclonal antibodies and anti-DWV

432 polyclonal antibodies confirmed the identity of the target proteins, indicating that
433 the DWV structural protein genes can be expressed in a prokaryotic system.

434 Comparing the codon usage in *E. coli*, we found many rare codons in the wild
435 DWV structural protein genes, and CAI values of the three target genes were only
436 approximately 0.2; this likely results in lower expression yields—even expression
437 failure—in *E. coli*. Codon optimization can improve protein production via
438 optimization of translation elongation, and previous reports have shown that a
439 codon-optimization strategy can improve the expression level of genes in many
440 species (*Chu et al., 2018; Hu et al., 2019; Nieuwkoop et al., 2019; Sun et al.,*
441 *2017*). In this study, the rare codons of DWV *VP1*, *VP2*, and *VP3* were replaced
442 with the most highly preferred codons, and the GC content was changed to
443 approximately 70%. In addition, the AT-rich fragment was removed to avoid
444 premature translation termination. After optimization, the CAI value of the three
445 genes reached approximately 0.95. To avoid the impact of tag proteins on the
446 spatial conformation of the recombinant protein, we selected pET28a (+) as the
447 expression vector because the molecular weight of the His-tag protein is only
448 approximately 0.8 kDa. SDS-PAGE showed that optimized *roVP1*, *roVP2*, and
449 *roVP3* were efficiently expressed in *E.coli*. Prokaryotic expression offers many
450 advantages, such as simple manipulation, relatively low capital costs, and fitting
451 mass production (*Liu et al., 2018*), and serves as a convenient method for obtaining
452 large numbers of recombinant proteins; however, protein sequences of VP1, VP2,
453 and VP3 probably exist as potential glycosilation sites as per online software
454 analysis (http://www.cbs.dtu.dk/services/NetNGlyc/), and the influence of
455 potential glycosilation sites on the immunogenicity requires further research.

456 Research has indicated that structural proteins of the virus not only play an
457 important role in viral invasion and replication but also have excellent
458 immunogenicity and that they are frequently selected as candidates for the
459 development of therapeutic antibodies (*Huo et al., 2018; Li et al., 2014; Stachyra*
460 *et al., 2016; Wang et al., 2017*). Compared with vertebrate immune systems, honey
461 bee immune pathways lack acquired immunity (*Bull et al., 2012*) and cannot
462 directly generate specific antibodies in response to an antigen. We therefore hope
463 to prepare the antibody against DWV by the mammal in the present study, and

464 humoral immunity is thought to be critical to evaluate the immunogenicity of the
465 three recombinant proteins. Our results showed that among the three recombinant
466 proteins, roVP3 induced the highest levels of specific IgG in the serum. IL-2 and
467 INF-γ are mainly secreted by Th1 cells, which promote cellular immune responses,
468 and IL-4 and IL-10 are mainly secreted by Th2 cells, which promote humoral
469 immune responses (*Wang et al., 2017; Zheng et al., 2019*). Comparing SI values
470 and and cytokines, we speculate that *roVP2* has a strong effect on cellular immune
471 responses and that *roVP3* can induce a strong humoral immune response in the
472 mice, although all the three recombinant proteins could stimulate cellular and
473 humoral immune responses.

474   In the challenge test, all the anti‑roVP1/2/3‑antisera could confer to the
475 pupae protection against DWV, which indicated that antisera against recombinant
476 protein of the mice possess the ability of neutralizing virus. Although co-injection
477 with anti-DWV or roVP1/2/3-antisera could reduce DW levels, whether they
478 prevent development of DWV infection need further research. In the
479 previous research, the C-terminal extension of VP3 protein folds into a globular
480 protruding (P) domain, exposed on the surface of the virion, which contains five
481 Asp-His-Ser residues, and the P domain may participate in receptor-binding or
482 provide the protease, lipase, or esterase activity required for entry of the virus into
483 a host cell (*Škubník et al., 2017*), and anti‑*roVP3*‑antisera show the most
484 superior viru‑neutralizing ability in challenge test; thus, we speculated that
485 anti‑*roVP3*‑antisera inhibits virus entry into target cells by the prevention of
486 conformational changes within P domain or the inhibition of receptor binding.
487 These results of the challenge test provide a new idea for development of a
488 treatment strategy against DWV.

489

490

491 **CONCLUSION**

492   In summary, the present study has shown for the first time that the DWV
493 structural proteins *VP1, VP2,* and *VP3* can be efficiently expressed in *E. coli* using
494 a codon-optimization strategy. Based on the results of mice immunization

495 experiments and challenge test, we found that the recombinant proteins *roVP3* and
496 *roVP2* have excellent immunogenicity in mice. After the virus were incubated with
497 the specific antibodies against DWV capsid proteins, virus copies from challenged
498 pupae reduced significantly on quantitative real-time RT-PCR detection in the
499 challenge test, which indicated that the specific antibodies against DWV capsid
500 proteins could neutralize DWV. Thus, they are promising candidate immunogens
501 for the development of therapeutic antibodies. Our research provides a novel
502 pathway for exploiting anti-DWV biological drugs and may aid further research
503 concerning the effects of DWV on honey bees.
504
505

506 **References**
507 **Bailey L, Ball BV. 1991.** Honey bee pathology (2nd Ed.). Academic Press.
508 London, United Kingdom: 113 **DOI http://dx.doi.org/10.9774/GLEAF.978-1-**
509 **909493-38-4_2**
510 **Benaets K, Van Geystelen A, Cardoen D, De Smet L, de Graaf DC, Schoofs L,**
511 **Wenseleers T. 2017.** Covert deformed wing virus infections have long-term
512 deleterious effects on honeybee foraging and survival. Proceedings of the Royal
513 Society B: Biological Sciences **284(1484):** 20162149 **DOI**
514 **10.1098/rspb.2016.2149**
515 **Bowen-Walker PL, Martin SJ, Gunn A. 1999.** The Transmission of Deformed
516 Wing Virus between Honeybees. (*Apis mellifera L.*) by the Ectoparasitic
517 MiteVarroa jacobsoniOud. Journal of invertebrate pathology **73(1):** 101-106 **DOI**
518 **10.1006/jipa.1998.4807**
519 **Bradford EL, Christie CR, Campbell EM, Bowman AS. 2017.** A real-time PCR
520 method for quantification of the total and major variant strains of the deformed
521 wing virus. PLoS One, **12(12)**: e0190017 **DOI 10.1371/journal.pone.0190017**
522 **Budge GE, Pietravalle S, Brown M, Laurenson L, Jones B, Tomkies, V,**
523 **Delaplane KS. 2015.** Pathogens as predictors of honey bee colony strength in
524 England and Wales. PLoS One **10(7):** e0133228 **DOI**
525 **10.1371/journal.pone.0133228**

526 **Bull JC, Ryabov EV, Prince G, Mead A, Zhang C, Baxter LA, Chandler D.**
527 **2012.** A strong immune response in young adult honeybees masks their increased
528 susceptibility to infection compared to older bees. PLoS pathogens **8(12):**
529 e1003083 **DOI 10.1371/journal.ppat.1003083**

530 **Capucci L, Rossi C. 2006.** Molecular and biological characterization of deformed
531 wing virus of honeybees (*Apis mellifera L.*). Journal of virology **80(10):** 4998-5009
532 **DOI 10.1128/JVI.80.10.4998-5009.2006**

533 **Chen, Y P, Higgins JA, Feldlaufer MF. 2005.** Quantitative Real-Time Reverse
534 Transcription-PCR Analysis of Deformed Wing Virus Infection in the Honeybee
535 (*Apis mellifera L.*). Applied and Environmental Microbiology**, 71(1),** 436–441
536 **DOI 10.1128/aem.71.1.436-441.2005**

537 **Chu C, Zhang W, Li J, Wan, Y, Wang Z, Duan R, Hao Q. 2018.** A Single
538 Codon Optimization Enhances Recombinant Human TNF-α Vaccine Expression in
539 *Escherichia coli*. BioMed research international **2018:** 1-8 **DOI**
540 **10.1155/2018/3025169**

541 **Dalmon A, Desbiez C, Coulon M, Thomasson M, Le Conte Y, Alaux C, Moury**
542 **B. 2017.** Evidence for positive selection and recombination hotspots in deformed
543 wing virus (DWV). Scientific reports **7:** 41045 **DOI**

544 **De Smet L, Ravoet J, de Miranda JR, Wenseleers T, Mueller MY, Moritz RF,**
545 **De Graaf DC. 2012.** BeeDoctor, a versatile MLPA-based diagnostic tool for
546 screening bee viruses. PLoS One **7(10):** e47953 **DOI**
547 **10.1371/journal.pone.0047953**

548 **Francis RM, Nielsen SL, Kryger P. 2013.** Varroa-Virus Interaction in Collapsing
549 Honey Bee Colonies. PloS One 8: e0057540
550 **DOI 10.1371/journal.pone.0057540**

551 **Fink AL, Williams KL, Harris E, Alvine TD, Henderson T, Schiltz J, Bradley**
552 **DS. 2017.** Dengue virus specific IgY provides protection following lethal dengue
553 virus challenge and is neutralizing in the absence of inducing antibody dependent
554 enhancement. PLoS neglected tropical diseases **11(7):** e0005721 **DOI**
555 **10.1371/journal.pntd.0005721**

556 **Gao CY, Xu TT, Zhao QJ, Li CL. 2015.** Codon optimization enhances the
557 expression of porcine β-defensin-2 in Escherichia coli. Genet Mol Res **14(2):**
558 4978-4988 **DOI 10.4238/2015.may.12.1**

559 **Garibaldi LA, Steffan-Dewenter I, Winfree R, Aizen MA, Bommarco R,**
560 **Cunningham SA, Bartomeus I. 2013.** Wild pollinators enhance fruit set of crops
561 regardless of honey bee abundance. Science **339(6127):** 1608-1611 **DOI**
562 **10.1126/science.1230200**

563 **Ghosh S, Malik YS, Kobayashi N. 2017.** Therapeutics and immunoprophylaxis
564 against noroviruses and rotaviruses: the past, present, and future. Current drug
565 metabolism **19(3):** 170-191 **DOI 10.2174/1389200218666170912161449**

566 **Gisder S, Möckel N, Eisenhardt D, Genersch E. 2018.** In vivo evolution of viral
567 virulence: switching of deformed wing virus between hosts results in virulence
568 changes and sequence shifts. Environmental microbiology **20(12):** 4612-4628 **DOI**
569 **10.1111/1462-2920.14481**

570 **Hu H, Dai S, Wen A, Bai X. 2019.** Efficient Expression of Xylanase by Codon
571 Optimization and Its Effects on the Growth Performance and Carcass
572 Characteristics of Broiler. Animals **9(2):** 65 **DOI 10.3390/ani9020065**

573 **Huo Y, Wan X, Ling T, Wu J, Wang W, Shen S. 2018.** Expression and
574 purification of norovirus virus like particles in *Escherichia coli* and their
575 immunogenicity in mice. Molecular immunology 93: 278-284 **DOI**
576 **10.1016/j.molimm.2017.07.014**

577 **Jahangiri A, Owlia P, Rasooli I, Salimian J, Derakhshanifar E, Naghipour**
578 **Erami A, Darvish Alipour Astaneh S. 2019.** Specific egg yolk antibodies (IgY)
579 confer protection against Acinetobacter baumannii in a murine pneumonia model.
580 Journal of Applied Microbiology **126(2):** 624-632 **DOI 10.1111/jam.14135**

581 **Jamnikar-Ciglenecki U, Pislak Ocepek M, Toplak I. 2018.** Genetic Diversity of
582 Deformed Wing Virus from *Apis mellifera* carnica (Hymenoptera: Apidae) and
583 Varroa Mite (Mesostigmata:Varroidae). Journal of economic entomology **112(1):**
584 11-19 **DOI 10.1093/jee/toy312**

585 **Kevill JL, de Souza FS, Sharples C, Oliver R, Schroeder DC, Martin SJ. 2019.**
586 DWV-A Lethal to Honey Bees (*Apis mellifera*): A Colony Level Survey of DWV

587   Variants (A, B, and C) in England, Wales, and 32 States across the US. Viruses

588   **11(5):** 426 **DOI 10.3390/v11050426**

589   **Koziy RV, Wood SC, Kozii IV, van Rensburg CJ, Moshynskyy I, Dvylyuk I,**

590   **Simko E. 2019.** Deformed Wing Virus Infection in Honey Bees (*Apis mellifera L.*).

591   Veterinary pathology **56(4):** 636-641 **DOI 10.1177/0300985819834617**

592   **Lamp B, Url A, Seitz K, Eichhorn J, Riedel, C, Sinn LJ, Rümenapf T. 2016.**

593   Construction and rescue of a molecular clone of deformed wing virus (DWV).

594   PloS one **11(11):** e0164639 **DOI 10.1371/journal.pone.0164639**

595   **Lanzi G, De Miranda JR, Boniotti MB, Cameron CE, Lavazza A, De Miranda**

596   **JR, Genersch E. 2010.** Deformed wing virus. Journal of invertebrate pathology

597   **103:** S48-S61 **DOI 10.1016/j.jip.2009.06.012**

598   **Li X, Jing K, Wang X, Li Y, Zhang M, Li Z, Xu Y. 2016.** Protective effects of

599   chicken egg yolk antibody (IgY) against experimental Vibrio splendidus infection

600   in the sea cucumber (Apostichopus japonicus). Fish & shellfish immunology **48:**

601   105-111 **DOI 10.1016/j.fsi.2015.11.024**

602   **Li YX, Zhao H, Cao RY, Deng YQ, Han JF, Zhu SY, Qin CF. 2014.**

603   Recombinant tandem multi-linear neutralizing epitopes of human enterovirus 71

604   elicited protective immunity in mice. Virology journal **11(1):** 79 **DOI**

605   **10.1186/1743-422X-11-79**

606   **Liu Y, Huang H. 2018.** Expression of single-domain antibody in different systems.

607   Applied microbiology and biotechnology **102(2):** 539-551 **DOI 10.1007/s00253-**

608   **017-8644-3**

609   **Mahdy SE, Liu S, Su L, Zhang X, Chen H, Pei X, Wang C. 2019.** Expression

610   of the VP1 protein of FMDV integrated chromosomally with mutant Listeria

611   monocytogenes strain induced both humoral and cellular immune responses.

612   Applied microbiology and biotechnology **103(4):** 1919-1929 **DOI**

613   **10.1007/s00253-018-09605-x**

614   **Mansouri M, Mousavy SJ, Ehsaei Z, Nazarian S, Zali MR, Moazzeni SM.**

615   **2013.** The codon-optimization of cfaE gene and evaluating its high expression

616   capacity and conserved immunogenicity in *Escherichia coli*. Biologicals **41(3):**

617   169-175 **DOI 10.1016/j.biologicals.2013.01.002**

618 **Mordecai GJ, Wilfert L, Martin SJ, Jones IM, Schroeder DC. 2016.** Diversity
619 in a honey bee pathogen: first report of a third master variant of the Deformed
620 Wing Virus quasispecies. The ISME journal **10(5):** 1264 **DOI**
621 **10.1038/ismej.2015.178**

622 **Natsopoulou ME, Mc Mahon DP, Doublet V, Frey E, Rosenkranz P, Paxton**
623 **RJ. 2017.** The virulent, emerging genotype B of Deformed wing virus is closely
624 linked to overwinter honeybee worker loss. Scientific reports **7(1):** 5242 **DOI**
625 **10.1038/s41598-017-05596-3**

626 **Nieuwkoop T, Claassens NJ, van der Oost J. 2019.** Improved protein production
627 and codon optimization analyses in *Escherichia coli* by bicistronic design.
628 Microbial biotechnology **12(1):** 173-179 **DOI 10.1111/1751-7915.13332**

629 **Ojha R, Nandani, R, Prajapati VK. 2019.** Contriving multiepitope subunit
630 vaccine by exploiting structural and nonstructural viral proteins to prevent
631 Epstein–Barr virus ‐ associated malignancy. Journal of cellular physiology **234(5):**
632 6437-6448 **DOI 10.1002/jcp.27380**

633

634

635 **Škubník K, Nováček J, Füzik T, Přidal A, Paxton RJ, Plevka P. 2017.**
636 Structure of deformed wing virus, a major honey bee pathogen. Proceedings of the
637 National Academy of Sciences **114(12):** 3210-3215 **DOI**
638 **10.1073/pnas.1615695114**

639 **Stachyra A, Redkiewicz P, Kosson P, Protasiuk A, Góra-Sochacka A, Kudla**
640 **G, Sirko A. 2016.** Codon optimization of antigen coding sequences improves the
641 immune potential of DNA vaccines against avian influenza virus H5N1 in mice
642 and chickens. Virology journal **13(1):** 143-153 **DOI 10.1186/s12985-016-0599-y**

643 **Sun H, Li J, Liu GZ, Yin K, Cui Y, Xiao T, Wei QK. 2017.** Expression of
644 codon-optimized TgMIC16 in three *Escherichia coli* strains. 3 Biotech **7(4):** 270
645 **DOI 10.1007/s13205-017-0885-4**

646 **Sun L, Li M, Fei D, Wang J, Li L, Mingxiao M. 2018.** Preparation and
647 application of egg yolk antibodies against Chinese sacbrood virus infection.
648 Frontiers in microbiology **9:** 1814 **DOI 10.3389/fmicb.2018.01814**

649 **Tehel A, Vu Q, Bigot D, Gogol-Döring A, Koch P, Jenkins C, Paxton R. 2019.**
650 The Two Prevalent Genotypes of an Emerging Infectious Disease, Deformed Wing
651 Virus, Cause Equally Low Pupal Mortality and Equally High Wing Deformities in
652 Host Honey Bees. Viruses **11(2):** 114 **DOI 10.3390/v11020114**
653 **Tian J, Yan Y, Yue Q, Liu X, Chu X, Wu N, Fan Y. 2017.** Predicting
654 synonymous codon usage and optimizing the heterologous gene for expression in *E.*
655 *coli*. Scientific reports **7(1):** 9926 **DOI 10.1038/s41598-017-10546-0**
656 **Wang H, Shan S, Wang S, Zhang H, Ma L, Hu L, Zhu, R. 2017.** Fused IgY Fc
657 and Polysaccharide Adjuvant Enhanced the Immune Effect of the Recombinant
658 VP2 and VP5 Subunits—A Prospect for Improvement of Infectious Bursal Disease
659 Virus Subunit Vaccine. Frontiers in microbiology **8:** 2258 **DOI**
660 **10.3389/fmicb.2017.02258**
661 **Wang Q, Mei C, Zhen H, Zhu J. 2012.** Codon preference optimization increases
662 prokaryotic cystatin expression. Journal of Biomedicine and Biotechnology **2012:**
663 732017 **DOI 10.1155/2012/732017**
664 **Xie Y, Li H, Qi X, Ma Y, Yang B, Zhang S, Li Z. 2019.** Immunogenicity and
665 protective efficacy of a novel foot-and-mouth disease virus empty-capsid-like
666 particle with improved acid stability. Vaccine **37(14):** 2016-2025 **DOI**
667 **10.1016/j.vaccine.2019.02.032**
668 **Yin L, Chen L, Luo Y, Lin L, Li Q, Du Y, Zhou Q. 2019.** Recombinant fiber-2
669 protein protects Muscovy ducks against duck adenovirus 3 (DAdV-3). Virology
670 **526:** 99-104 **DOI 10.1016/j.virol.2018.10.011**
671 **Zhao Y, Heerman M, Peng W, Evans JD, Rose R, DeGrandi-Hoffman G, Su S.**
672 **2019.** The dynamics of Deformed wing virus concentration and host defensive
673 gene expression after varroa mite parasitism in honey bees, *Apis mellifera*. Insects
674 **10(1):** 16 **DOI 10.3390/insects10010016**
675 **Zheng B, Lou D, Ding J, Zhuo X, Ding H, Kong Q, Lu S. 2019.** GRA24-Based
676 DNA Vaccine Prolongs Survival in Mice Challenged With a Virulent Toxoplasma
677 gondii Strain. Frontiers in immunology **10:** 418 **DOI 10.3389/fimmu. 2019.**
678 **00418**
679

Figure 1

Expression and purification of the recombinant proteins by SDS-PAGE analysis in *E.coli*.

A, B, and C represent the recombinant proteins *roVP1*, *roVP2*, and *roVP3*, respectively. Lane 1; protein weight marker. Lane 2-4; induced *E. coli* BL21 (DE3) of the corresponding plasmids after 6 h with 0.1 mM, 0.25 mM, and 0.5 mM IPTG, respectively. Lane 5, uninduced *E. coli* BL21 (DE3) of the corresponding plasmids as control. Lane 6; purification of the corresponding recombinant proteins.
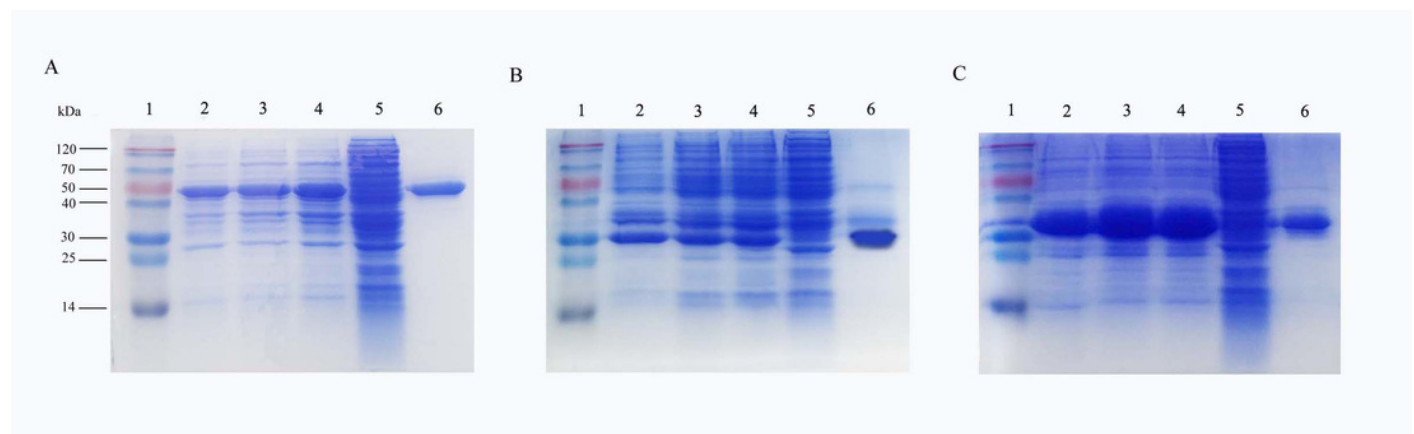
Figure 2

Western blot identification of the recombinant proteins with the anti–His tag antibody and mouse anti–DWV polyclonal antibody.

A, B, and C represent *roVP1*, *roVP2*, and *roVP3*, respectively. Lane 1; anti–His tag antibody was used as primary antibody. Lane 2; mouse anti–DWV polyclonal antibodies as primary antibody. Lane 3; negative control (NC), the serum of healthy mice.
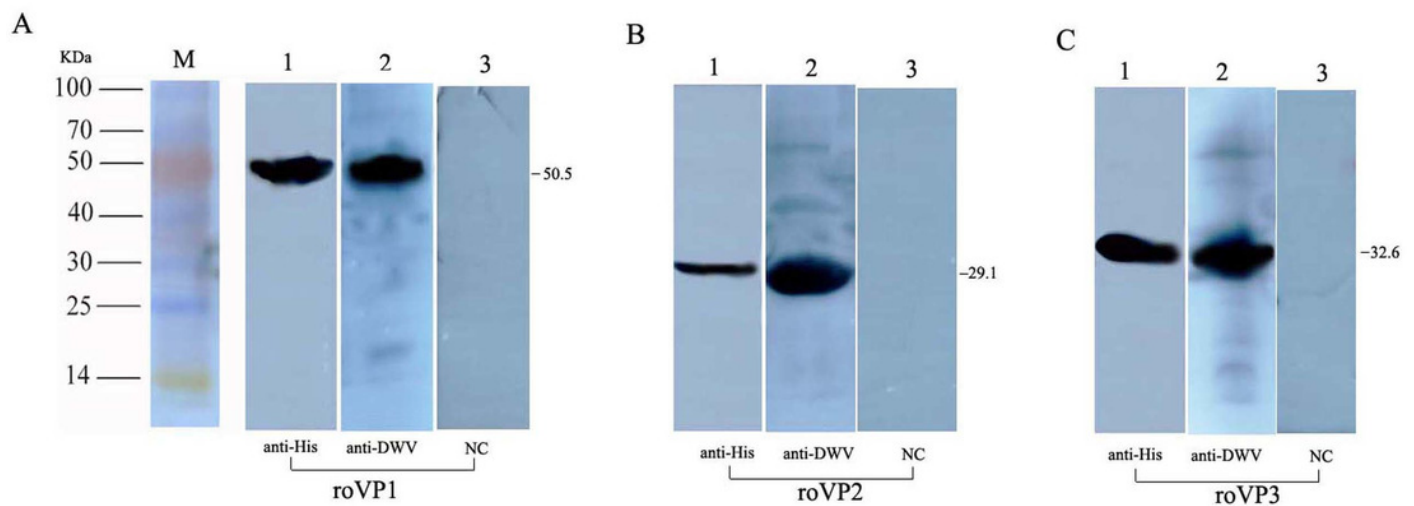
Figure 3

Specific IgG antibodies in serum of the immunized mice

The OD_{450} value of total IgG were detected on 0, 2, 4, and 6 weeks post-vaccination. Data are expressed as the mean ± SD (n = 5) values. *Significantly different compared with the control group (P<0.05). **Significant differences between three groups immunized with recombinant proteins (P<0.05).
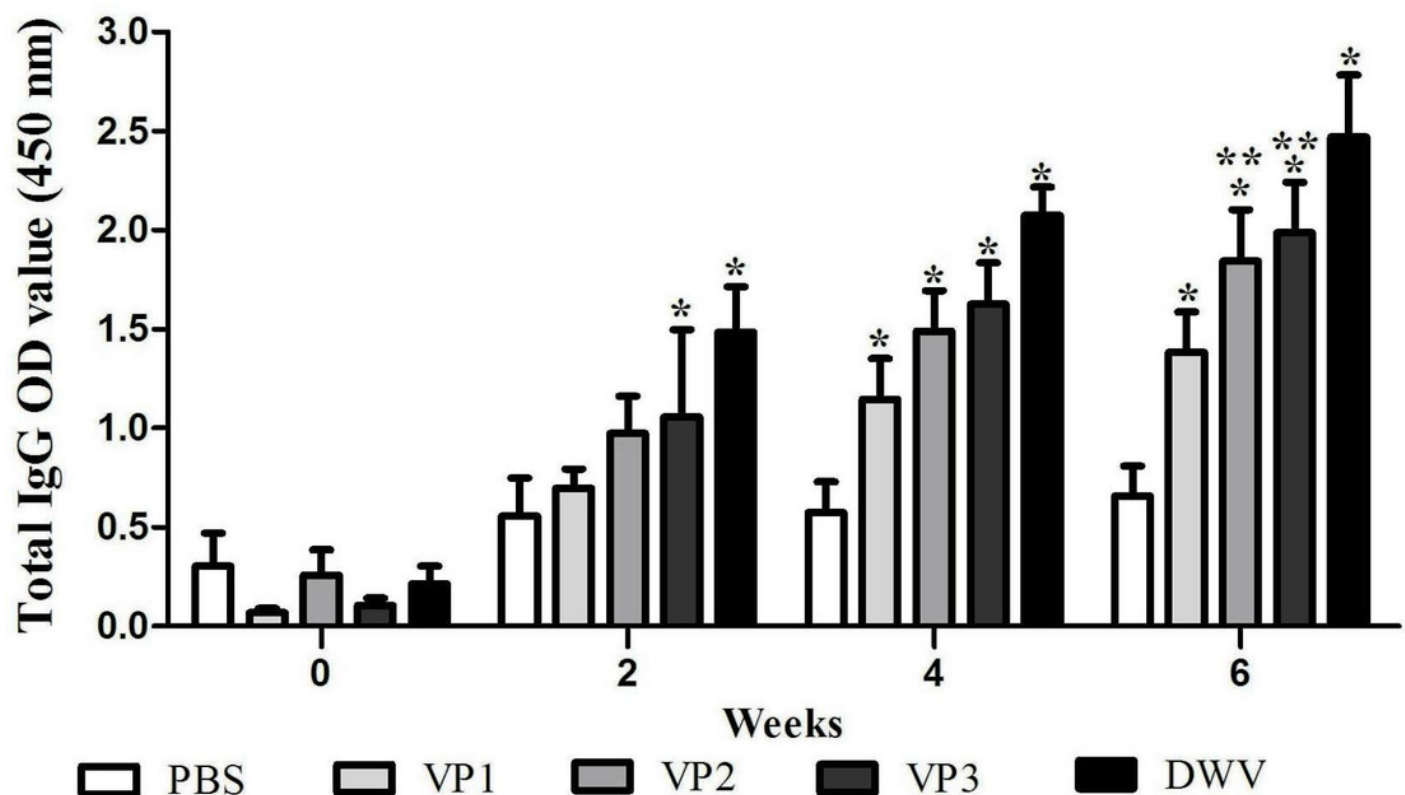
Figure 4

Lymphocyte proliferation responses of immunized mice

The value of Stimulation index (SI) were calculated at 6 weeks post-vaccination. Data are expressed as the mean ± SD (n = 5) values. *Significantly different than the control group ($P<0.05$).
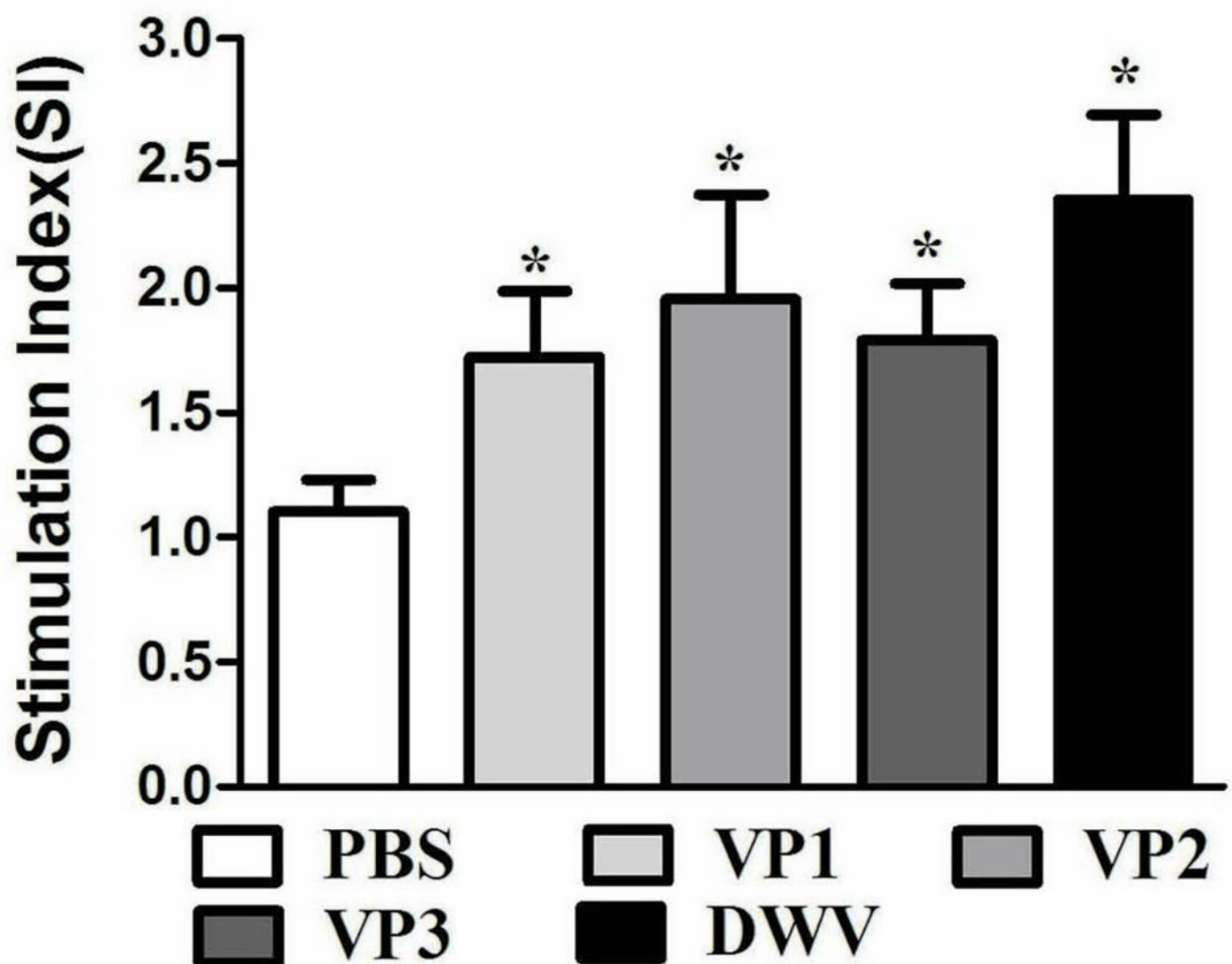
Figure 5

Cytokine response in sera of immunized mice

A, B, C and D represent the levels of cytokines IL-2, IL-4, IL-10, and IFN-γ by ELISA, respectively. Data are expressed as the mean ± SD (n = 5) values. *Significantly different compared with the control group (*P*<0.05). **Significant differences between three groups immunized with recombinant proteins (*P*<0.05).
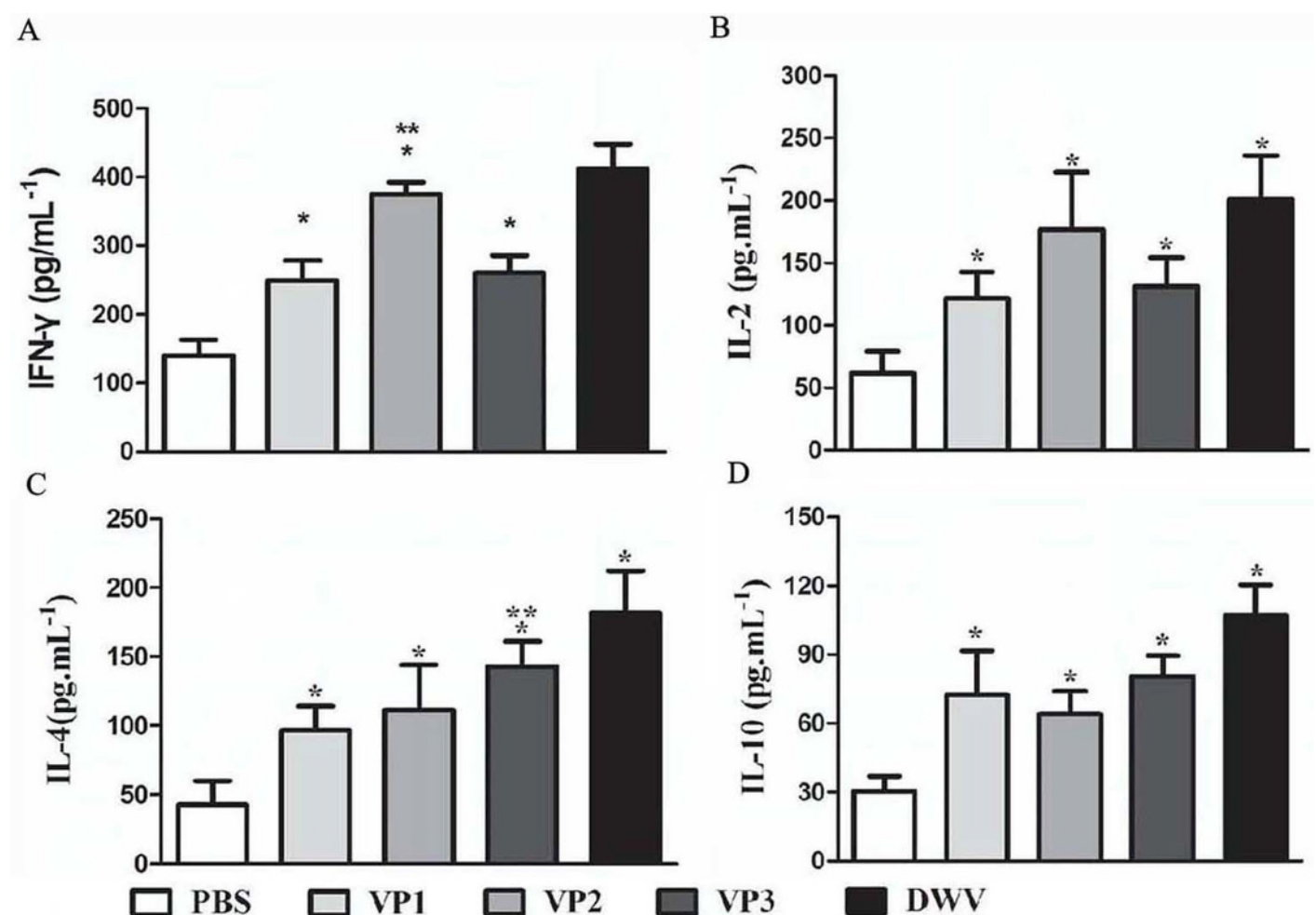
Figure 6

Relative normalized DWV of the honeybee pupae

The quantification of DWV titer in the samples was performed by the real time qRT-PCR, and the relative normalized DWV titer was determined as the DWV titer after normalization with the reference gene Actin, and the relative DWV titers of the pupae were assessed by calculating delta Ct values ($\Delta Ct = Ct_{(DWV)} - Ct_{(actin)}$).*Significantly different compared with the virus-only group ($P<0.05$). **Significant differences between three groups immunized with recombinant proteins ($P<0.05$).